# NONVOLATILE STATE CONFIGURATION OF NANO-WATT PARAMETRIC ISING SPINS THROUGH FERROELECTRIC HAFNIUM ZIRCONIUM OXIDE MEMS VARACTORS

Nicolas Casilli<sup>1</sup>, Onurcan Kaya<sup>1</sup>, Tahmid Kaisar<sup>2</sup>, Benyamin Davaji<sup>1</sup>, Philip X.-L. Feng<sup>2</sup>, and Cristian Cassella<sup>1</sup>

<sup>1</sup>Northeastern University, Boston, MA 02115, USA and <sup>2</sup>University of Florida, Gainesville, FL 32611, USA

## **ABSTRACT**

This work reports on an Ising system formed by two artificial spins and relying, for the first time, on a ferroelectric MEMS device to permanently configure the spins' interactions to ferromagnetic or anti-ferromagnetic. These spins, consisting of two parametric oscillators (POs) built from off-the-shelf components, are driven by the same 2MHz ("pump") signal and are coupled through a series LC-network with resonance frequency (fc) formed by two inductors and a microfabricated hafnium zirconium oxide (HZO) MEMS varactor. We show that leveraging the nonvolatile ferroelectric memory characteristic of the HZO varactor allows a shift of  $f_C$  to a lower or to a higher value than ~1MHz based on HZO polarization state, triggering nonvolatile ferromagnetic or anti-ferromagnetic interactions without consuming power for the spincoupling during the system operation. These features, together with the exceptionally low power threshold of the POs, makes the reported Ising system consume the least power-per-spin ( $\sim 600 nW$ ) reported to date.

# **KEYWORDS**

MEMS, Ising Machines, Parametric Oscillators, Ferroelectric Devices, Ferromagnetic Spins

## INTRODUCTION

Modern applications in science, economics, and engineering would benefit from solving a variety of nondeterministic polynomial-time (NP) hard problems [1]. For instance, there is a great interest in developing strategies to more efficiently allocate healthcare resources [2], maximize expected returns of investments [3], and allocate network resources in highly trafficked, rapidly changing channel configurations [4], [5]. These NP-hard problems are also used extensively in the algorithms underlying the capability of artificial intelligence (AI) and machine learning (ML) programs [6]. Unfortunately, many of these problems are left unsolved since the existing von-Neumann computing architectures are unable to solve them in a tractable amount of time. Quantum-inspired adiabatic hardware-solvers known as Ising machines (IMs) have emerged, generating new resources to find the solution for NP-hard problems by identifying the ground-state of a corresponding Ising Hamiltonian [1], [7]-[9]. Among the demonstrated IMs, those using resistively coupled subharmonic-injection-locked (SHIL) oscillators as spins [1], becoming popular because of robust manufacturability through complementary-metal-oxidesemiconductor (CMOS) fabrication processes and easier re-programmability through monolithically integrated CMOS-circuits. Nonetheless, the power-per-spin

consumed by SHIL oscillator IMs is set by the mW-range power levels needed to sustain the oscillation of their spins, trigger the injection-locking regime, and implement the spin-coupling, making SHIL-based IMs hardly usable to solve problems requiring  $10^3$  spins or more. We addressed this limitation by demonstrating: i) CMOS-compatible Ising spins made of POs driven by the same  $\sim 2MHz$  pump signal and engineered to consume only nW-power; and ii) a coupling network, unbiased during the spin operation, composed of two inductors and a ferroelectric HZO capacitor.

In this paper, a novel nonvolatile resonance coupling architecture capable of providing permanent state configuration to a system of two coupled Ising spins is presented. This architecture exploits the memory dynamics of ferroelectric HZO to create a permanent, re-configurable shift in the resonance frequency of the coupling network to set the interaction of the coupled POs as ferromagnetic or anti-ferromagnetic. In the first section, the principle of operation of the POs and the fabrication flow of the tunable HZO MEMS varactor are introduced. The operating principle, experimental methods, and experimental results of the system of two coupled POs, along with simulated solutions for several *4-node* Max-Cut problems, are reported in the following section. In the conclusions, future research directions are discussed.

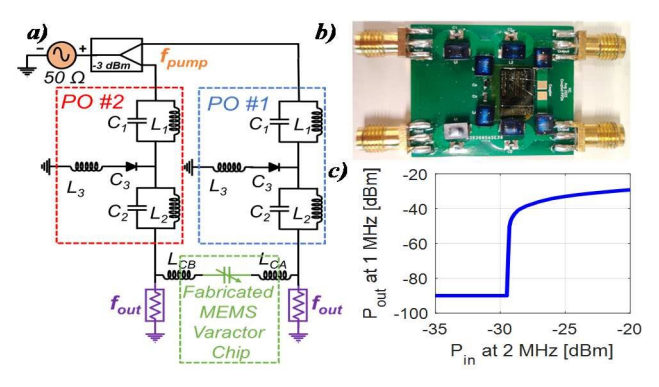


Fig. 1: a) Schematic view of the reported Ising system using two coupled POs and the HZO varactor in their coupling network; b) Top-view picture of the constructed PCB hosting the reported Ising system, showing the HZO device after wire-bonding; c) Measured trend of the POs' output power at 1MHz vs. their input power at 2MHz. The model numbers for the components are as follows: C3: SMV1236-079LF (26.75pF, tuning range = 36%),  $L_1$ : 1812LS-334XLJC (330 $\mu$ H),  $L_2$ : 1812LS-474XLJC (470 $\mu$ H),  $L_3$ : 1812LS-334XLJC (330 $\mu$ H),  $C_1$ : GRM1555C1H750JA01 (75pF),  $C_2$ : GRM1555C1R70WA01 (0.7pF),  $L_{CA}$ : 1812LS-824XLJC (820 $\mu$ H),  $L_{CB}$ : 1812LS-684XLJC (680 $\mu$ H), HZO Varactor: 15.5pF, tuning range = 9%.

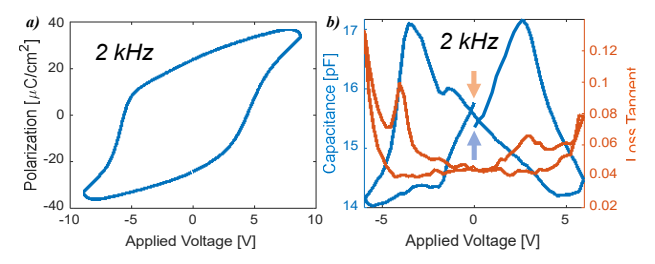


Fig. 2: Left) Measured polarization loop (PE-loop) by PUND method and C-V curve (right) of the HZO varactor. Both are measured at a frequency of 2kHz. Evidently, the device shows two different capacitance values at 0V in its two polarization states. These 0V capacitance values are marked with a blue and orange arrow to indicate whether the contribute to an fc that results in a ferromagnetic or anti-ferromagnetic interaction, respectively.

### **METHODS**

The coupled two-spin Ising system presented in this paper features PO designs relying on a varactor-based parametric frequency divider that exhibits a perioddoubling mechanism under a particular operational region [10]. This region is activated through a supercritical bifurcation for an input power  $(P_{in})$  exceeding a certain power threshold  $(P_{th})$ , resulting in an output frequency  $(f_{out})$ that is one half of the frequency of the driving signal  $(f_{pump})$ [11]. This subharmonic output signal provides the basis for the artificial spins, as the spins for this PO-based topology are represented by the subharmonic output phase of a single PO converging to 0 or  $\pi$  with respect to the output phase of a reference PO [1]. Recent theoretical studies have shown that the strategic selection of the components of a PO and its operational frequency greatly reduce the resultant  $P_{th}$ based on the satisfaction of four resonant conditions governing the equivalent impedance of the branches in the PO circuit topology [10].

In essence, these resonant conditions provide a structure for intelligently directing the emergent nonlinear subharmonic oscillations to the output of the oscillator. Particularly, i) the series of  $L_2$ ,  $C_2$ ,  $L_3$ , and  $C_3$  must seriesresonate at  $f_{out}$ ; ii) the series of  $L_1$ ,  $C_1$ ,  $L_3$ , and  $C_3$  must series-resonate at  $f_{pump}$ ; iii)  $L_1$  and  $C_1$  must behave as a bandstop filter at  $f_{out}$ ; and iv)  $L_2$  and  $C_2$  must behave as a bandstop filter at  $f_{pump}$  [10]. These conditions inform the design of the POs used in this paper to produce the lowest ever recorded  $P_{th}$  (-32dBm) for a PO constructed entirely with off-the-shelf lumped components and operating with  $f_{pump} = 2MHz$ . To create these POs, 3 inductors ( $L_1 =$  $330\mu H$ ,  $L_2 = 470\mu H$ , and  $L_3 = 330\mu H$ ), 2 capacitors ( $C_I =$ 75pF and  $C_2 = 0.7pF$ ), and 1 varactor ( $C_3 = 26.75pF$ , tuning range = 36%) are used. As observed, using POs with a  $P_{th}$ this low permits to create IMs with up to  $10^6$  spins while consuming less than IW. This offers a marked improvement of scalability compared to the maximum IMsize that can be reasonably exploited with the available resistively coupled SHIL-based IMs.

To couple the POs, a network comprised of two offthe-shelf inductors and an in-house fabricated HZO MEMS varactor is employed [12]. This coupling network exhibits a resonance frequency ( $f_C$ ) proximate to  $f_{out}$ . The coupled PO circuit topology, constructed system, threshold plot characterizing the performance of the coupled POs, and a list of the lumped components are shown in Fig. 1. Within the coupling network, the HZO MEMS varactor was designed to operate at 15.5pF, and the lumped inductors are selected as  $820\mu H$  and  $680\mu H$  to set  $f_C$  to be as close as possible to the  $f_{out}$  of the POs. Using the positive-up, negative-down (PUND) method, the PE-loop and C-V curve of the HZO varactor have been measured and are reported in Fig. 2. The measured characteristics of the device demonstrate a clear difference in nominal capacitance and polarization, even at 0V, depending on the polarization state of the HZO film. This ferroelectric hysteresis behavior permits to exercise unique memory dynamics that allow our Ising system to operate without having to consume power due to leakage during the Ising system operation to maintain the desired programmable coupling weight between the spins.

By exploiting this phenomenon, we show that setting the polarization state of the HZO varactor before activating the spins generates a nonvolatile change of  $f_C$ , permanently varying the spin interaction between ferromagnetic and anti-ferromagnetic such that no power is needed for the spin coupling during the operation of the Ising system. Particularly, the HZO varactor exhibits different nominal capacitance values at  $\partial V$  depending on its polarization (e.g., positively or negatively polarized), making  $f_C$  lower or higher than the POs' oscillation frequency of fout. For fc  $< f_{out}$ , the synchronization of the two POs exhibits out-ofphase output signals, realizing an anti-ferromagnetic interaction. The opposite case produces in-phase output signals, implementing a ferromagnetic interaction. As shown in the next section, the change in HZO polarization state produces a significant enough variation in the capacitance of the device at OV that the resonance

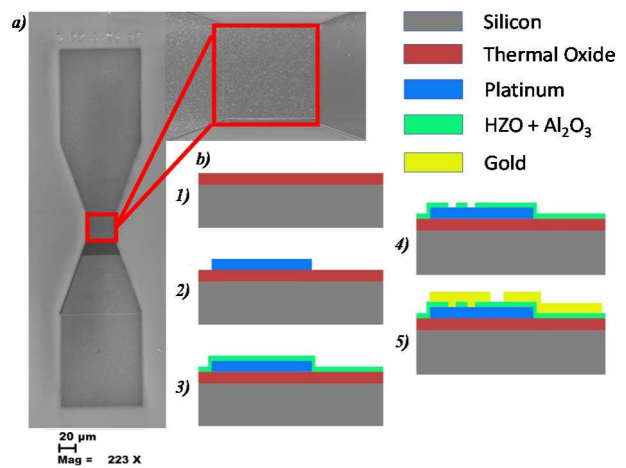


Fig. 3: a) Scanned-Electron-Microscope (SEM) picture of the fabricated HZO varactor device and magnification on the parallel plate capacitance structure. a) Fabrication flow we followed to build the HZO varactor used in this work. We started with 1) silicon wafer with a 150nm thermal oxide as the substrate; 2) sputtered and patterned 100nm platinum with lift-off; 3) deposited 20nm HZO and 3nm Al<sub>2</sub>O<sub>3</sub> using ALD; 4) created vias using a dry plasma etch; and 5) deposited 150nm of gold using E-beam evaporation. After step 5), the deposition samples are annealed in a rapid thermal processor in an N<sub>2</sub> environment at 400°C for 40 seconds.

frequency of the coupling network can shift above or below  $f_{out}$  and permanently trigger a specific Ising coupling state without the need for an additional applied voltage.

The HZO MEMS varactor is designed as a typical parallel plate capacitor, with 100nm of platinum and 150nm of gold sandwiching a 20nm thin film of HZO and 3nm of Al<sub>2</sub>O<sub>3</sub> deposited using atomic layer deposition (ALD). At such low thicknesses, the HZO exhibits the ferroelectric properties which enable the tuning of the capacitor and its consequent hysteresis relationship with applied voltage. In fact, at lower thicknesses (10nm), HZO becomes antiferroelectric, providing a rich set of functionalities in the thin-film regime, meaning that this material offers many exciting possibilities for future applications relevant to tunability [12]. The fabrication process used to create these varactors is shown and described in Fig. 3.

#### RESULTS AND SIMULATIONS

We have validated our theoretical predictions by fabricating an HZO varactor [12] and wire-bonding it onto a printed-circuit-board (PCB) hosting two identical coupled POs [10] driven by a 2MHz input signal and exhibiting the lowest power threshold (600nW) ever demonstrated for electronic POs. Firstly, the HZO material is excited several times through the pads of the PCB using the PUND method to apply a +5V 1.2kHz pulse and ensure that the initial state of the HZO during experimentation is positively polarized. Then, the two POs are fed by a single signal generator (model-number: Tektronix TSG 4104A) providing pump power at -20dBm, above the system  $P_{th}$  of -29dBm which is 3dBm higher than the threshold of a single PO since we are using the same pump signal to activate both POs. The POs' output waveforms are extracted in the time domain using an oscilloscope (model-number: InfiniiVision DSOX6004A). The driving signal is applied three separate times for each HZO polarization state to demonstrate permanence and consistency of the Ising behavior. As seen in Fig. 4, the POs exhibit in-phase output voltages, corresponding to a ferromagnetic interaction, when the HZO is positively polarized. The POs are then totally disconnected from the oscilloscope and signal generator and a -5V 1.2kHz signal is applied to the HZO varactor using PUND to negatively polarize the HZO device. After this step, a similar analysis is conducted and it is measured that the output phases of the POs are shifted by  $\pi$  with respect to each other, indicating an antiferromagnetic interaction. Again, the POs are fully disconnected from the measurement instruments and the ferroelectric varactor is polarized positively using a +5V1.2kHz signal. The POs are driven again using the same signal at 2MHz and their output phases are shown to be inphase. Fig. 4 shows a system-level depiction of the transitions of the HZO polarization states performed in this experiment and the corresponding output waveforms of the POs for each of those states.

Furthermore, this experiment shows that the HZO polarization state, through the mechanism of changing  $f_C$ , offers a nonvolatile, permanent state configuration of the PO spins to ferromagnetic or anti-ferromagnetic without the need for a constantly applied bias voltage. Since the polarization state of the HZO is retained even at  $\theta V$  DC bias, the power cost of this system is only what is necessary

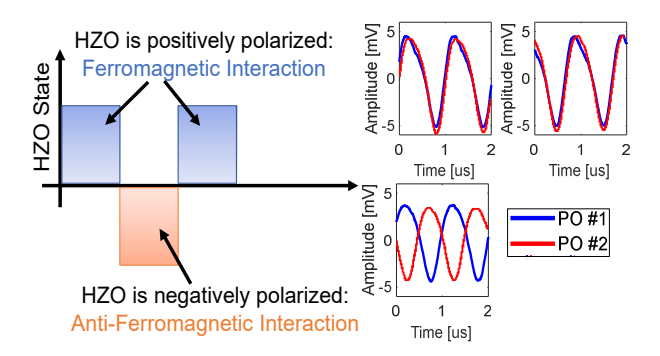


Fig. 4: Schematic view of the followed experimental procedure and measured output waveforms of the two POs for both polarization states of the HZO varactor. Two waveforms are reported for the case of the positively polarized HZO varactor in order to show the repeatability of the reported technique in controlling the interaction of the two Ising spins. With a positive polarization, the output waveforms of the coupled POs exhibit in-phase (ferromagnetic) behavior. When the HZO varactor is negatively polarized, the system exhibits anti-phase (anti-ferromagnetic) behavior.

to drive the POs above their input power threshold. This method of coupling offers exciting possibilities for the development of a larger, CMOS-compatible IM with an easily re-programmable binary-weighted coupling scheme consuming only RF power.

In order to benchmark the performance of our artificial spins compared to the state-of-the-art, it is useful to evaluate the cost-per-spin of the oscillators used in IM topologies. Furthermore, a table (Table 1) has been prepared delineating the operational frequency and power consumption per spin for several different types of oscillators used in existing IMs. It is worth emphasizing that this power per spin metric considers only the amount of power needed to excite the oscillators, and it does not consider any DC biasing voltage that needs to be applied to maintain any desired coupling weight. Upon a quick inspection, the RF power cost of using POs is one order of magnitude lower than the next best type of oscillator, demonstrating the immense potential of PO-based IMs to solve CO problems of larger complexity than those realistically solvable by IMs relying on other types of oscillators.

To show that PO-based systems, like the one presented in this work, can indeed be used as Ising solvers for NPhard problems, we analytically show how a network of POs

*Table 1. Comparison with other artificial spins.* 

Type of Oscillator	Operational Frequency	Power per Spin	Reference
LC	1 MHz	20.8mW	[1]
LC	50 kHz	/	[7]
Ring	1 GHz	23μW	[8]
Ring	118 MHz	41μW	[9]
PO	2 MHz	600nW	This work

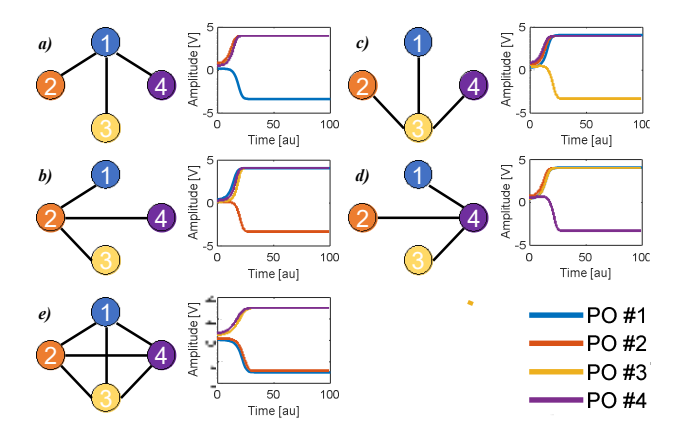


Fig. 5: Several 4-node graphs where a) all POs are connected to PO #1; b) all POs are connected to PO #2; c) all POs are connected to PO #3; d) all POs are connected to PO #4; and e) all POs are connected to all other POs. In each case, the simulated voltage outputs match with the correct solution for the Max-Cut problem, demonstrating the successful capability of POs-based Ising solvers to find the solution of NP-hard problems.

effectively solves several selected 4-node Max-Cut problems [7] (Fig. 5). With our analytical model, we have verified the correctness of each spin phase solution through a comparison with solutions produced by other IMs and the solution derived using a Max-Cut approximate solution algorithm for the same set of problem graphs [7], [13]. Furthermore, it is demonstrated that by changing the value of  $f_C$  between two coupled POs, a specific Ising interaction can be permanently configured. A PO-based IM relying on this coupling architecture and using the type of POs reported in this paper is a promising path forward to addressing the problem-size, miniaturization, and reprogrammability concerns currently plaguing other oscillator-based IMs and IMs in general.

#### CONCLUSIONS

In this paper, a novel approach to Ising spin state configuration is proposed based on the nonvolatile memory characteristics of the ferroelectric HZO MEMS varactor used for coupling the artificial spins. The proposed architecture is theoretically described and verified experimentally by measuring the output phases of the POs when driven with a 2MHz signal at different polarization states of the 20nm HZO film at 0V DC bias. It has been shown that the HZO film deterministically affects the phase convergence of the Ising system, triggering ferromagnetic or anti-ferromagnetic spin interactions depending on its current polarization state due to the resultant shift of the  $f_C$  of the coupling network relative to the output frequency of the POs. These experimental results, paired with a simulation framework for higher order Ising systems of coupled POs, will enable the development of exciting new capabilities for miniaturized, low power, CMOS-compatible, and re-programmable IMs.

# **ACKNOWLEDGEMENTS**

We thank the support from the National Science Foundation CCF-FET program (Grants #2103351 & #2103091).

## REFERENCES

- [1] T. Wang and J. Roychowdhury, "Oscillator-based Ising Machine," 2017.
- [2] Jeffrey. E. Arle and K. W. Carlson, "Medical diagnosis and treatment is *NP-complete*," *J. Exp. Theor. Artif. Intell.*, vol. 33, no. 2, pp. 297–312, Mar. 2021.
- [3] R. Orús, S. Mugel, and E. Lizaso, "Quantum computing for finance: Overview and prospects," *Rev. Phys.*, vol. 4, p. 100028, Nov. 2019.
- [4] A. Samuylov *et al.*, "Characterizing Resource Allocation Trade-Offs in 5G NR Serving Multicast and Unicast Traffic," *IEEE Trans. Wirel. Commun.*, vol. 19, no. 5, pp. 3421–3434, May 2020.
- [5] C. She, R. Dong, W. Hardjawana, Y. Li, and B. Vucetic, "Optimizing Resource Allocation for 5G Services with Diverse Quality-of-Service Requirements," in 2019 IEEE Global Communications Conference (GLOBECOM), Waikoloa, HI, USA, Dec. 2019, pp. 1–6.
- [6] C. J. Hillar and L.-H. Lim, "Most Tensor Problems Are NP-Hard," *J. ACM*, vol. 60, no. 6, pp. 1–39, Nov. 2013.
- [7] J. Chou, S. Bramhavar, S. Ghosh, and W. Herzog, "Analog Coupled Oscillator Based Weighted Ising Machine," *Sci. Rep.*, vol. 9, no. 1, p. 14786, Dec. 2019.
- [8] W. Moy, I. Ahmed, P. Chiu, J. Moy, S. S. Sapatnekar, and C. H. Kim, "A 1,968-node coupled ring oscillator circuit for combinatorial optimization problem solving," *Nat. Electron.*, vol. 5, no. 5, pp. 310–317, May 2022.
- [9] I. Ahmed, P.-W. Chiu, W. Moy, and C. H. Kim, "A Probabilistic Compute Fabric Based on Coupled Ring Oscillators for Solving Combinatorial Optimization Problems," *IEEE J. Solid-State Circuits*, vol. 56, no. 9, pp. 2870–2880, Sep. 2021.
- [10] H. M. E. Hussein, M. A. A. Ibrahim, G. Michetti, M. Rinaldi, M. Onabajo, and C. Cassella, "Systematic Synthesis and Design of Ultralow Threshold 2:1 Parametric Frequency Dividers," *IEEE Trans. Microw. Theory Tech.*, vol. 68, no. 8, pp. 3497–3509, Aug. 2020.
- [11] H. M. E. Hussein, M. Rinaldi, M. Onabajo, and C. Cassella, "A chip-less and battery-less subharmonic tag for wireless sensing with parametrically enhanced sensitivity and dynamic range," *Sci. Rep.*, vol. 11, no. 1, p. 3782, Dec. 2021.
- [12] V. Gund *et al.*, "Multi-level Analog Programmable Graphene Resistive Memory with Fractional Channel Ferroelectric Switching in Hafnium Zirconium Oxide," in *2022 EFTF/IFCS*, Paris, France, Apr. 2022, pp. 1–4.
- [13] M. X. Goemans and D. P. Williamson, "Improved approximation algorithms for maximum cut and satisfiability problems using semidefinite programming," *J. ACM*, vol. 42, no. 6, pp. 1115–1145, Nov. 1995.

# **CONTACT**

\*N. Casilli, casilli.n@northeastern.edu